Available online at www.sciencedirect.com

ScienceDirect

IFAC PapersOnline CONFERENCE PAPER ARCHIVE

IFAC PapersOnLine 56-3 (2023) 409–414

Free Vibration Modeling of Power Line Conductors

Ranhee Yoon * **Erdi Gulbahce** ** **Oumar Barry** ***

* *Virginia Polytechnic Institute and State University, Blacksburg, VA 24061 USA (e-mail: ranheey@vt.edu).*

** *Virginia Polytechnic Institute and State University, Blacksburg, VA 24061 USA & KTO Karatay University, Konya, Turkey (e-mail: erdigulbahce@vt.edu)*

*** *Virginia Polytechnic Institute and State University, Blacksburg, VA 24061 USA (e-mail: obarry@vt.edu)*

Abstract: This paper investigates a suitable model for a power line conductor to explore its free vibration characteristics. For this, we compare the Euler–Bernoulli beam model of the conductor against the string model of the conductor via experimental and analytical vibration analyses. The effects of conductor parameters such as flexural rigidity, diameter, length, and tension on the natural frequencies of different modes are explored through parametric studies. We observe that the Euler–Bernoulli beam model of the conductor is a more realistic approach to examining the conductor's free vibration characteristics as compared to a string model.

Keywords: Aeolian vibration, power line, conductor modeling, Euler–Bernoulli beam model, string model

1. INTRODUCTION

The US power grid consists of 7 million miles of transmission and distribution lines. Since power lines are one of the essential infrastructures in our society, it is vital to avoid or mitigate any damage to power lines. One of the phenomena plaguing power lines is wind-induced vibrations. Wind-induced vibrations can give rise to repetitive and enormous damage to power lines through excessive vibrations and hence, has to be mitigated (Barry (2014); Kakou (2021)). To have a better understanding of the vibration characteristics of power lines, it is essential to have a conductor model which is close to the realistic scenario. Also, deciding on the conductor model from the existing models, such as beam and string models, for the analysis is crucial. This is the focus of the current work.

Mechanical vibrations can cause undesirable effects on structures, damaging the components of mechanical systems and further reducing the life of structures. Therefore, it has been a subject of investigation for many researchers. Aeolian vibrations are one of the phenomena which occur in structures such as bridges, cables, and aero-elastic structures due to fluid-structure interactions. Many studies were performed in the early 1980s to explore the response of structures towards aeolian vibrations (Ramey and Silva (1981); Basu et al. (1981); Roughan (1983); Nigol et al. (1985); Tsui (1988)).

Transmission lines are one of the structures susceptible to aeolian vibrations and have been a subject of research for many years. Kraus and Hagedorn (1991); Barbieri et al. (2004); Barbieri et al. (2017) investigated the dynamical behavior of transmission lines during aeolian vibrations. Oliveira and Freire (1994) presented a dynamical model for aeolian vibrations of single conductors. Nigol et al. (1985) designed the optimal aeolian vibration dampers and discussed the optimal locations of the damper.

George H. Stockbridge were the first to develop the Stockbridge damper (Stockbridge (1925)) to suppress aeolian vibrations in power lines effectively. Further, the Stockbridge damper characteristics were researched by Markiewicz (1995); Vecchiarelli (1998) to optimize the damper parameters. Later on, Barry et al. (2013) investigated the vibration response of a conductor with an attached Stockbridge damper and identified that the effectiveness of Stockbridge dampers depends on their location, mass, and excitation frequency. Wang et al. (2021) examined the sensitivity analysis of the parameters of the Stockbridge damper and optimized the damper location. However, the Stockbridge damper fixed on a conductor, is practically impossible to guarantee reasonable performance at every wind frequency (Kakou (2021)).

One of the recent trends in suppressing the aeolian vibrations is using a mobile robot equipped with a Stockbridge damper. As shown in Fig. 1, Self-Powered Autonomous Robot (SPAR) is being developed (Barry and Bukhari (2017); Bukhari et al. (2018); Kakou et al. (2021); Kakou and Barry (2021); Choi et al. (2022)). This mobile robot works by finding an anti-node (the point of maximum amplitude of a conductor for a given mode) and moves to the anti-node to effectively reduce the vibration amplitude of the conductor. Accordingly, finding an anti-node of a conductor is one of the important processes in the research involving SPAR. Since the vibration of a conductor depends on the wind velocity (Barry (2010); Kakou (2021)), an understanding of the aeolian vibrations of a conductor is an essential step toward the optimum development of

10.1016/j.ifacol.2023.12.058

SPAR. Further, for the vibration analysis, selecting the conductor model from the existing models (such as beam and string models) for real-life scenarios is crucial.

Fig. 1. Conceptual design model of SPAR (Kakou (2021)).

However, to the authors' knowledge, no studies guide the selection of the conductor model for practical analysis with different parameters of the conductor. In this paper, a power line conductor is modeled as a beam and string model and are compared with the experimental results in low tension and low length condition. For this, the effects of conductor design parameters such as flexural rigidity, diameter, length, and tension on the beam and string models are analyzed through parametric studies to understand the conductor's vibration characteristics.

The rest of the paper is organized as follows. Section 2 presents the theoretical background and analytical methods for this work. A detailed discussion of the experiments is presented in Section 3, followed by results and discussion in Section 4. Finally, some conclusions are drawn in Section 5.

2. THEORETICAL BACKGROUND AND METHODOLOGY

Fig. 2. Structure of a conductor (Electrical Technology (2020)).

Table 1. Conductor Parameters.

Parameter	**Value**	
Mass per unit length	ρA	0.3493 kg/m
Length	L	7.32 m
Tension	T	1330 N
Diameter	d	14.4 x10^{-3} m
Flexural Rigidity	EI	149.86 Nm^2

In transmission lines, conductors are constructed with individual wires packed tightly together in several layers, as shown in Fig. 2. In this study, All Aluminum Conductor (AAC) is used for analytical and experimental studies, and the parameters of the conductor are listed in Table 1. Due to multiple layers of wires in the conductor, it is difficult to get a governing equation of motion incorporating the complex structure of the conductor. Therefore, in this paper, we assume the conductor as a cylindrical body with a homogeneous structure over the entire cross-sectional area (Vecchiarelli (1998)). Accordingly, the governing equation of motion for a conductor is given by (Barbieri et al. (2004))

$$EI\frac{\partial^4 w(x,t)}{\partial x^4} + \rho A\frac{\partial^2 w(x,t)}{\partial t^2} - T\frac{\partial^2 w(x,t)}{\partial x^2} = f(x,t) \quad (1)$$

where, $f(x,t)$ is a uniformly distributed external load, w is the transverse displacement of the conductor relative to its equilibrium position, x is the coordinate along the length of the conductor, T is the conductor tension, ρA is the mass per unit length, A is the cross-sectional area, E is the modulus of elasticity, I is the moment of inertia of the cross-section about the neutral axis, and EI the flexural rigidity. We emphasize that the above governing equation of motion is based on the Euler-Bernoulli beam.

Accordingly, the boundary conditions for our system are, $w = 0$ at $x = 0$, $w = 0$ at $x = L$, $\partial^2 y/\partial x^2 = 0$ at $x = L$. When considering the conductor as an Euler-Bernoulli beam, the theoretical natural frequencies can be obtained by (Claren and Diana (1969); Vecchiarelli (1998); Barry (2010)).

$$\omega_n = \frac{n}{2L}\sqrt{\frac{T}{\rho A} + \left(\frac{n\pi}{L}\right)^2 \frac{EI}{\rho A}} \quad (2)$$

where w_n is the n^{th} natural frequency in Hz, and n is an integer denoting the mode number ($n = 1, 2, ...$).

Furthermore, if the stiffness of the conductor is very small and can be ignored, the flexural rigidity in Eq. 2. becomes zero ($EI = 0$). Hence, a conductor with a very small value of flexural rigidity behaves like a string, and the natural frequencies of a conductor can be obtained as

$$\omega_f = \frac{n}{2L}\sqrt{\frac{T}{\rho A}}. \quad (3)$$

Having obtained the analytical expressions for the natural frequencies of the conductor as a beam and string model, we next present a detailed discussion of the experiments.

3. EXPERIMENTS

The experiments for the modal analysis are primarily focused on defining modal parameters using two methods, viz., non-contact by using a laser vibrometer and contact through an accelerometer in a laboratory environment. The experiments are performed using a vibrometer (Polytec PSV-500), a signal conditioner (Bruel & Kjaer LDS LPA100 amplifier), an accelerometer (PCB Piezotronics YT352C34), and a modal hammer (Kistler). Also, the internal software of Polytec PSV-500 is used to interface with the hardware, record data, and post-process to define modal parameters. The experimental setup is illustrated schematically in Fig. 3, and is configured as shown in Fig. 4 in the laboratory.

The conductor is excited using the modal hammer, and the results are averaged after three repeated measurements per point. The four different Frequency Response Functions (FRF) are obtained using two points, (1) midpoint and (2) random point, as shown in Fig. 4. The two sensing devices used in the experiment, the accelerometer, and the vibrometer, are placed respectively at the midpoint

and random point of the conductor. The experiments are conducted by exciting the midpoint, H#1, (or random point H#2), and collecting the FRF through the accelerometer and vibrometer. This information is summarized in Table 2.

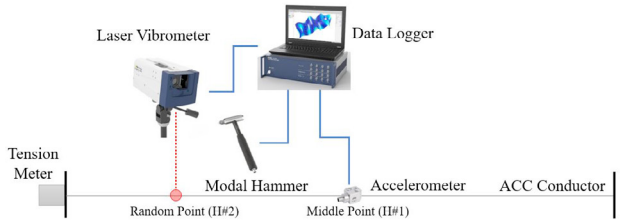

Fig. 3. Schematic illustration of the experimental setup.

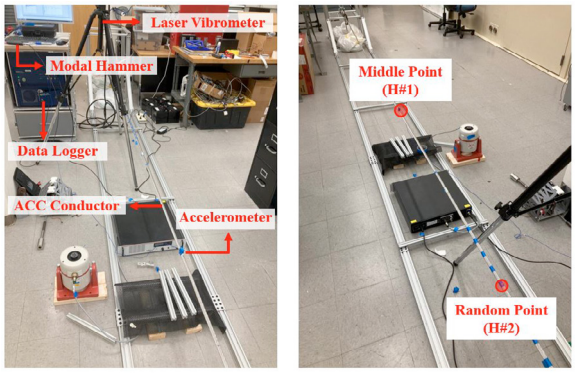

Fig. 4. Experimental setup.

Table 2. FRF determination points through experiments.

	Middle Point (H#1)	**Random Point (H#2)**
Accelerometer	H#1/ACC	H#2/ACC
Laser Vibrometer	H#1/VIB	H#2/VIB

4. RESULTS AND DISCUSSION

4.1 Analytical

The analytical study is performed by using the parameters of the conductor listed in Table 1 unless otherwise stated. The natural frequencies of the conductor for the first tenth mode ($n = 10$) are determined for the beam model and string model using Eqs. 2. and 3., respectively. Since the expression for the natural frequency contains the parameters of a conductor, such as flexural rigidity, diameter, length, and tension, these can be varied for the parametric analysis. We emphasize that flexural rigidity is a principal indicator of whether a conductor behaves like a string or a beam; therefore, we first start with the variation of natural frequencies for different values of flexural rigidity.

For flexural rigidity, $EI = 1$ Nm^2, the beam and the string model of the conductor have almost the same natural frequencies within 1% of error, as shown in Fig. 5. On the other hand, as the number of modes increases, the difference between the two models also increases rapidly. In particular, the trend of difference is convex until the flexural rigidity is 10 Nm^2 as shown in Fig. 6. However, after $EI = 100$ Nm^2, the trend of difference starts becoming concave, as shown in Fig. 7. In Fig. 8, when the flexural rigidity is 1000 Nm^2, the trend of the difference showed a perfect concave shape, which implies rapid growth in the difference for the first few modes followed by slow growth. Furthermore, from Fig. 8, we can observe that the difference between both models, which is only 6% in the first mode, becomes 74% in the tenth mode.

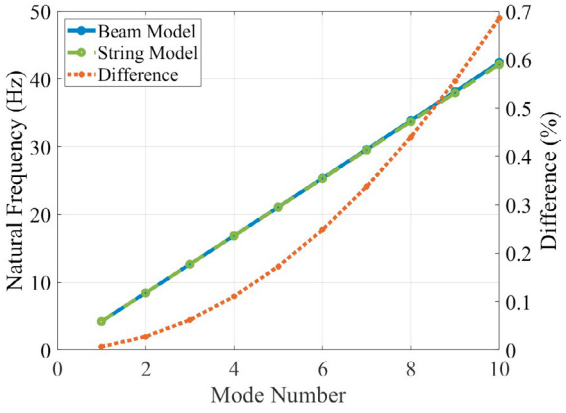

Fig. 5. Natural frequencies of the analytical beam model and analytical string model ($EI = 1$ Nm^2).

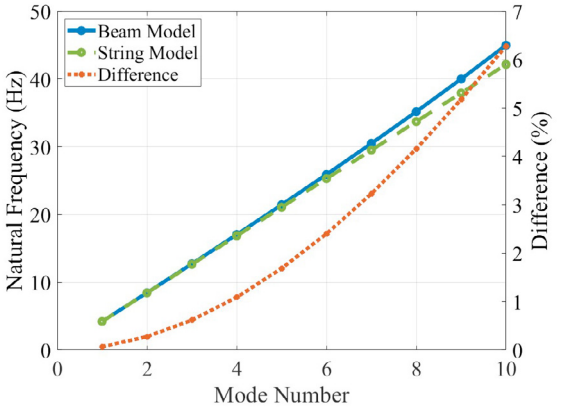

Fig. 6. Natural frequencies of the analytical beam model and analytical string model ($EI = 10$ Nm^2).

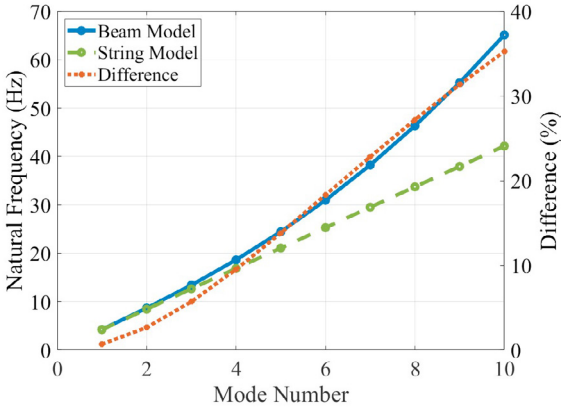

Fig. 7. Natural frequencies of the analytical beam model and analytical string model ($EI = 100$ Nm^2).

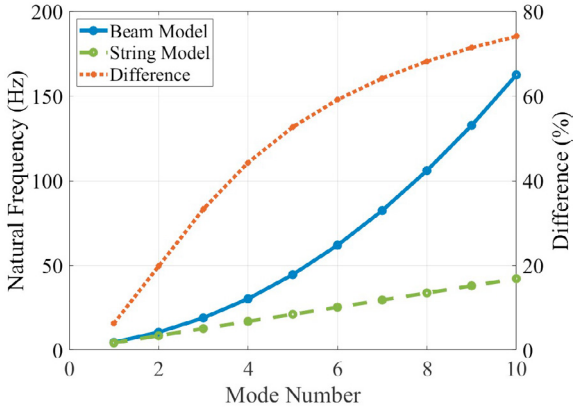

Fig. 8. Natural frequencies of the analytical beam model and analytical string model ($EI = 1000\ \mathrm{Nm}^2$).

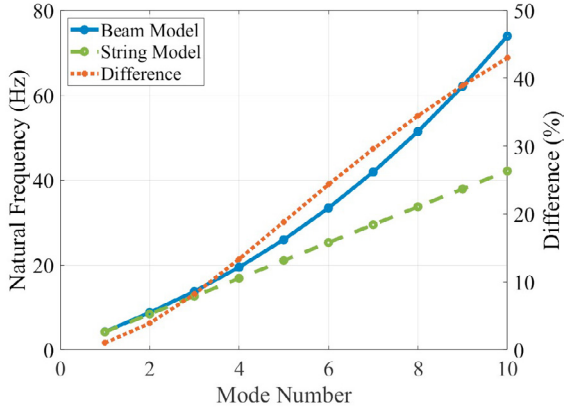

Fig. 9. Natural frequencies of the analytical beam model and analytical string model ($EI = 149.86\ \mathrm{Nm}^2$).

Figure 9 shows the variation of the natural frequency and difference with different modes for $EI = 149.86\ \mathrm{Nm}^2$ which is the value of the conductor used in the experiment. The beam model has a natural frequency of about 4 Hz to 26 Hz, and the string model has a natural frequency of about 4 Hz to 21 Hz, which further implies the maximum value of the difference to be around 43%.

For varying diameter, length, or tension, the change of the difference in natural frequency between the beam and the string model is shown in Figs. 10 to 12, respectively. For this analysis, the flexural rigidity is considered to be $EI = 149.86\ \mathrm{Nm}^2$ (experimental value). Figure 10 shows the difference between the natural frequencies of the two models with the change in conductor diameter from 1 to 20 mm and with different modes. The difference increases significantly after 14 mm diameter. Also, the higher mode shows a more significant difference, and the natural frequency of the tenth mode at a diameter of 20 mm has a difference of around 66%.

The effect of the length of the conductor is shown in Fig. 11. Unlike the case for the diameter, the difference is higher for the shorter length of the conductor. When the conductor length is longer than 10 m, the difference below the fifth mode between the two models is less than 10%, but the difference increases rapidly when the length is shorter than 10 m.

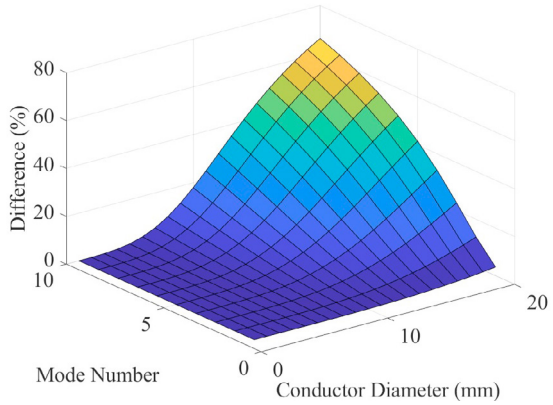

Fig. 10. Difference between the analytical beam model and analytical string model with diameter.

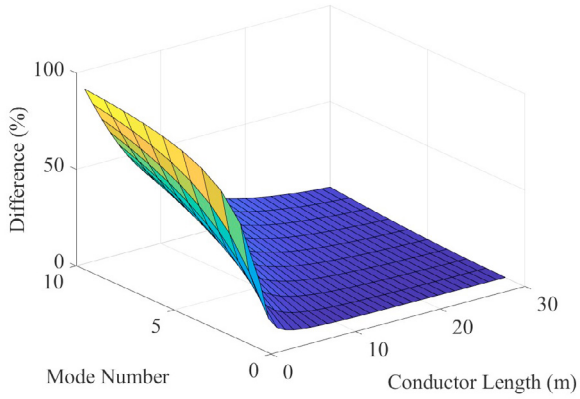

Fig. 11. Difference between the analytical beam model and analytical string model with length.

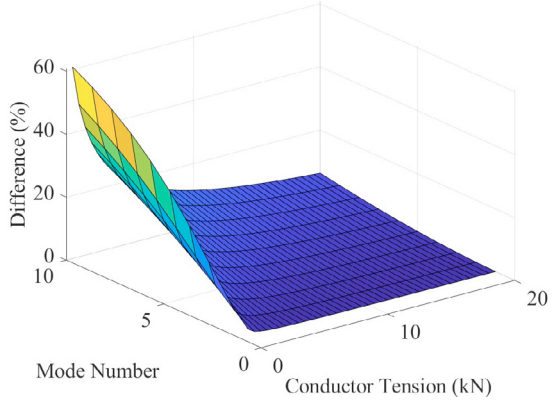

Fig. 12. Difference between the analytical beam model and analytical string model with tension.

The effect of tension on the difference between the natural frequencies for both models is shown in Fig. 12. Similar to the results for the length of the conductor, the difference in natural frequency increases as the tension decreases. Further, the difference becomes very large at $T = 2$ kN, and the maximum difference was calculated at approximately 60% for the tenth mode when the tension was 0.5 kN.

4.2 Experimental

The natural frequencies obtained from the experiment are compared with the analytical results to confirm the validity of the analytical study with the parameter values listed in Table 1. The natural frequencies of the first fifth modes are obtained through the experiment, and the results are compared against the analytical results. This comparison is shown in Fig. 13. The natural frequencies are identified in the range of 4 Hz to 24 Hz from the experimental results, 4 Hz to 26 Hz from the beam model, and 4 Hz to 21 Hz from the string model. It has been shown that the beam model has more similar natural frequencies to the experimental results than the string model, in particular for the second and third modes.

The natural frequencies from the analytic models (beam and string model) and the experimental are listed in Table 3. On comparing analytical results with the experimental results, the errors for each mode are calculated as, respectively, 6.61%, 1.87%, 1.36%, 4.11%, and 7.64% for the beam model, and 7.57%, 5.71%, 6.96%, 6.79%, and 12.66% for the string model. As the number of modes increases, the errors between the analytic models and the experimental results tend to increase. Figure 13 and Table 3 confirm that the beam model provides values closer to the experimental results than the string model for all natural frequencies.

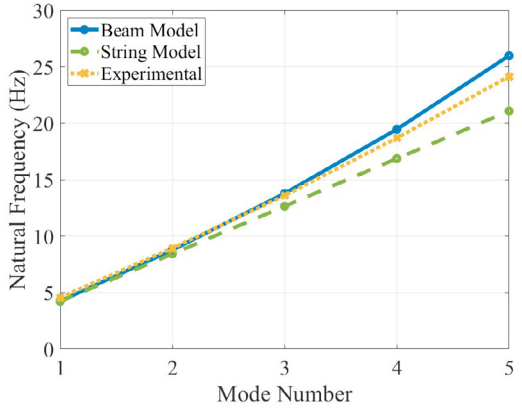

Fig. 13. Natural frequencies of the analytical models and the experiments.

Table 3. Natural frequencies from the analytical models and the experiments.

Mode	Beam (Hz)	String (Hz)	Experimental (Hz)
1	4.26 Hz	4.21 Hz	4.56 Hz
2	8.77 Hz	8.43 Hz	8.94 Hz
3	13.78 Hz	12.64 Hz	13.59 Hz
4	19.46 Hz	16.86 Hz	18.69 Hz
5	25.97 Hz	21.07 Hz	24.13 Hz

5. DISCUSSION

As the flexural rigidity increases, the difference between the beam and string models becomes larger. This suggests that if a conductor with high flexural rigidity is modeled as string, inaccurate results could lead to misinterpretation. Therefore, for the conductor with high flexural rigidity ($>$ 100 Nm^2), the conductor should be modeled as a beam to avoid any discrepancies between analytical and experimental results.

From the parametric studies, it can be confirmed that the difference between the beam and the string models increases as the diameter increases and as the length and tension decrease. Since the influence of each parameter showed a rapid change based on a specific value, it would be necessary to identify these points while modeling the conductor.

Furthermore, flexural rigidity, conductor diameter, conductor length, and conductor tension have a greater effect on the natural frequency as the number of modes increases. The influence of the parameters was relatively small up to about the third mode with the natural frequency within 10 Hz. If the higher frequency is the range of interest, these parameters should be treated more importantly.

From the experimental results, we can observe that the beam model is a more appropriate choice for modeling the conductor than the string model. Especially in the case of higher modes, such as second and third modes, the beam mode differs from the experimental results by 1% compared to the string model, where it differs by 6%. This observation can be attributed to the appearance of the term $EI(n\pi)^2/\rho AL^2$ in the natural frequency of the beam. In contrast, the natural frequency of the string does not take into account flexural rigidity. Since the conductor considered in the experiment has non-negligible flexural rigidity and a short span, the term $EI(n\pi)^2/\rho AL^2$ becomes significant and can not be ignored. Furthermore, the low tension of the conductor also increases the difference between a beam and a string model.

6. CONCLUSION

This work seeks to design an appropriate model of a power line conductor to study aeolian vibrations. For this, the conductor models based on the theoretical methodology of beam and string models were examined. In the analytical study, the influences of the parameters related to the natural frequency of a conductor, such as flexural rigidity, conductor diameter, conductor length, and conductor tension, were comparatively analyzed between the beam and the string model. We observed that as the flexural rigidity increased, the differences between the two models also increased at the higher modes. Furthermore, the high tension value and the long span caused low differences. As a result, the conductor parameters should be considered carefully while selecting the model for the conductor.

Furthermore, the analytical results were compared with the experimental results for the first five modes to validate our observations. These results showed that modeling a conductor based on a beam model is more compatible with experimental results in low tension and short span condition as predicted by analytical results.

This study contributes as a fundamental study to the research of aeolian vibrations of a power line conductor and would be helpful to analyze the effect of the mass of the mobile robot, SPAR, on the vibration of a conductor. Moreover, it could be a foundation for identifying the

relationship between the wind and the anti-node point of a conductor, which is essential for the development of SPAR.

ACKNOWLEDGEMENTS

This work is funded by National Science Foundation CAREER Award ECCS 1944032: Towards a Self-Powered Autonomous Robot for Intelligent Power Lines Vibration Control and Monitoring. Any opinions, findings, and conclusions or recommendations expressed in this material are those of the author(s) and do not necessarily reflect the views of the National Science Foundation.

REFERENCES

Barbieri, N., Calado, M.K.T., Mannala, M.J., de Lima, K.F., and Barbieri, G.d.S.V. (2017). Dynamical analysis of various transmission line cables. *Procedia engineering*, 199, 516–521.

Barbieri, N., de Souza Júnior, O.H., and Barbieri, R. (2004). Dynamical analysis of transmission line cables. part 1—linear theory. *Mechanical Systems and Signal Processing*, 18(3), 659–669.

Barry, O. (2010). Finite element analysis of a single conductor with a stockbridge damper under aeolian vibration'. *MASc, Mechanical Engineering, Ryerson University, Toronto, Canada*.

Barry, O. and Bukhari, M. (2017). On the modeling and analysis of an energy harvester moving vibration absorber for power lines. In *Dynamic Systems and Control Conference*, volume 58288, V002T23A005. American Society of Mechanical Engineers.

Barry, O., Oguamanam, D.C., and Lin, D.C. (2013). Aeolian vibration of a single conductor with a stockbridge damper. *Proceedings of the Institution of Mechanical Engineers, Part C: Journal of Mechanical Engineering Science*, 227(5), 935–945.

Barry, R.O. (2014). *Vibration Modeling and Analysis of a Single Conductor With Stockbridge Dampers*. Ph.D. thesis, University of Toronto.

Basu, S., Chi, M., et al. (1981). Analytical study for fatigue of highway bridge cables.

Bukhari, M.A., Barry, O., and Tanbour, E. (2018). On the vibration analysis of power lines with moving dampers. *Journal of vibration and control*, 24(18), 4096–4109.

Choi, A., Kakou, P.C., and Barry, O. (2022). Considerations for the testing and validation of a mobile damping robot for overhead power lines. In *International Design Engineering Technical Conferences and Computers and Information in Engineering Conference*, volume 86311, V010T10A026. American Society of Mechanical Engineers.

Claren, R. and Diana, G. (1969). Mathematical analysis of transmission line vibration. *IEEE Transactions on power apparatus and systems*, (12), 1741–1771.

Electrical Technology (2020). Types of electrical wires and cables. Https://www.electricaltechnology.org/2020/04/types-wires-cables.html (Accessed: 2023-03-31).

Kakou, P., Bukhari, M., Wang, J., and Barry, O. (2021). On the vibration suppression of power lines using mobile damping robots. *Engineering Structures*, 239, 112312.

Kakou, P.C. (2021). *Towards A Mobile Damping Robot For Vibration Reduction of Power Lines*. Ph.D. thesis, Virginia Tech.

Kakou, P.C. and Barry, O. (2021). Toward a mobile robot for vibration control and inspection of power lines. *ASME Letters in Dynamic Systems and Control*, 2(1), 011001.

Kraus, M. and Hagedorn, P. (1991). Aeolian vibrations: wind energy input evaluated from measurements on an energized transmission line. *IEEE Transactions on Power Delivery*, 6(3), 1264–1270. doi:10.1109/61.85875.

Markiewicz, M. (1995). Optimum dynamic characteristics of stockbridge dampers for dead-end spans. *Journal of sound and vibration*, 188(2), 243–256.

Nigol, O., Heics, R.C., and Houston, H.J. (1985). Aeolian vibration of single conductors and its control. *IEEE Transactions on Power Apparatus and Systems*, PAS-104(11), 3245–3254. doi:10.1109/TPAS.1985.318838.

Oliveira, A. and Freire, D. (1994). Dynamical modelling and analysis of aeolian vibrations of single conductors. *IEEE Transactions on Power Delivery*, 9(3), 1685–1693. doi:10.1109/61.311193.

Ramey, G. and Silva, J. (1981). An experimental evaluation of conductor aeolian fatigue damage mitigation by amplitude reduction. *IEEE Transactions on Power Apparatus and Systems*, (12), 4935–4940.

Roughan, J. (1983). Estimation of conductor vibration amplitudes caused by aeolian vibration. *Journal of Wind Engineering and Industrial Aerodynamics*, 14(1-3), 279–288.

Stockbridge, G. (1925). Vibration damper patent no. 1675391.

Tsui, Y. (1988). Modern developments in aeolian vibration. *Electric power systems research*, 15(3), 173–179.

Vecchiarelli, J. (1998). *Aeolian vibration of a conductor with a Stockbridge-type damper*. Ph.D. thesis.

Wang, Z., Li, H.N., and Song, G. (2021). Aeolian vibration control of power transmission line using stockbridge type dampers—a review. *International Journal of Structural Stability and Dynamics*, 21(01), 2130001.